Flexible liquid metal-filled metamaterial absorber on polydimethylsiloxane (PDMS)

Kenyu Ling, Kyeoungseob Kim, and Sungjoon Lim[*]

Laboratory of Electromagnetics and Optic, School of Electrical and Electronic Engineering, Chung-Ang University, Heukseok-Dong, Dongjak-Gu 156-756, Seoul, South Korea
[*]sungjoon@cau.ac.kr

Abstract: In this paper, we propose a novel flexible metamaterial (MM) absorber. The conductive pattern consists of liquid metal eutectic gallium indium alloy (EGaIn) enclosed in elastomeric microfluidic channels. Polydimethylsiloxane (PDMS) material is used as a supporting substrate. The proposed MM absorber is flexible because of its liquid metal and PDMS substrate. Numerical simulations and experimental results are presented when the microfluidic channels are filled with liquid metal. In order to evaluate the proposed MM absorber's performance, the fabricated absorber prototype is tested with rectangular waveguides. Almost perfect absorptivity is achieved at a resonant frequency of 8.22 GHz.

References and links

1. V. G. Veselago, "The electrodynamics of substances with simultaneously negative value of ε and μ," Sov. Phys. Usp. **10**(4), 509–514 (1968).
2. N. Fang, H. Lee, C. Sun, and H. Zhang, "Sub-diffraction-limited optical imaging with a silver superlens," Science **308**(5721), 534–537 (2005).
3. D. Schurig, J. J. Mock, B. J. Justice, S. A. Cummer, J. B. Pendry, A. F. Starr, and D. R. Smith, "Metamaterial electromagnetic cloak at microwave frequencies," Science **314**(5801), 977–980 (2006).
4. S. Enoch, G. Tayeb, P. Sabouroux, N. Guérin, and P. Vincent, "A metamaterial for directive emission," Phys. Rev. Lett. **89**(21), 213902 (2002).
5. N. I. Landy, S. Sajuyigbe, J. J. Mock, D. R. Smith, and W. J. Padilla, "Perfect metamaterial absorber," Phys. Rev. Lett. **100**(20), 207402 (2008).
6. H. Tao, C. Bingham, D. Pilon, K. Fan, A. Strikwerda, D. Shrekenhamer, W. Padilla, X. Zhang, and R. Averitt, "A dual band terahertz metamaterial absorber," J. Phys. D **43**(22), 225102 (2010).
7. S. Chen, H. Cheng, H. Yang, J. Li, X. Duan, C. Gu, and J. Tian, "Polarization insensitive and omnidirectional broadband near perfect planar metamaterial absorber in the near infrared regime," Appl. Phys. Lett. **99**(25), 253104 (2011).
8. P. K. Singh, K. A. Korolev, M. N. Afsar, and S. Sonkusale, "Single and dual band 77/95/110 GHz metamaterial absorbers on flexible polyimide substrate," Appl. Phys. Lett. **99**(26), 264101 (2011).
9. H. Tao, A. Strikwerda, K. Fan, C. Bingham, W. Padilla, X. Zhang, and R. Averitt, "Terahertz metamaterials on free-standing highly-flexible polyimide substrates," J. Phys. D Appl. Phys. **41**(23), 232004 (2008).
10. K. Iwaszczuk, A. C. Strikwerda, K. Fan, X. Zhang, R. D. Averitt, and P. U. Jepsen, "Flexible metamaterial absorbers for stealth applications at terahertz frequencies," Opt. Express **20**(1), 635–643 (2012).
11. D. Kim, D. Kim, S. Hwang, and J. Jang, "Surface relief structures for a flexible broadband terahertz absorber," Opt. Express **20**(15), 16815–16822 (2012).
12. J. So, J. Thelen, A. Qusba, G. J. Hayes, G. Lazzi, and M. D. Dickey, "Reversibly deformable and mechanically tunable fluidic antennas," Adv. Funct. Mater. **19**(22), 3632–3637 (2009).
13. S. Cheng, A. Rydberg, K. Hjort, and Z. Wu, "Liquid metal stretchable unbalanced loop antenna," Appl. Phys. Lett. **94**(14), 144103 (2009).
14. G. J. Hayes, J. So, A. Qusba, M. D. Dickey, and G. Lazzi, "Flexible liquid metal alloy (EGaIn) microstrip patch antenna," IEEE Trans. Antenn. Propag. **60**(5), 2151–2156 (2012).
15. S. Bhattacharya, A. Datta, J. M. Berg, and S. Gangopadhyay, "Studies on surface wettability of poly (dimethyl) siloxane (PDMS) and glass under oxygen-plasma treatment and correlation with bond strength," J. Microelectromech. Syst. **14**(3), 590–597 (2005).
16. S. Fallahzadeh, K. Forooraghi, and Z. Atlasbaf, A polarization-insensitive metamaterial absorber with a broad angular band" in Electrical Engineering (ICEE), 2012 20th Iranian Conference on Anonymous (2012).
17. D. R. Smith, D. C. Vier, T. Koschny, and C. M. Soukoulis, "Electromagnetic parameter retrieval from inhomogeneous metamaterials," Phys. Rev. E Stat. Nonlin. Soft Matter Phys. **71**(3 3 Pt 2B), 036617 (2005).

18. M. Safari, C. Shafai, and L. Shafai, "X-Band tunable frequency selective surface using MEMS capacitive loads," IEEE Trans. Antenn. Propag. **63**(3), 1014–1021 (2014).

1. Introduction

Metamaterials (MM) are artificial composite materials consisting of structural units considerably smaller than the wavelength of the incident electromagnetic wave. These artificial materials demonstrate certain extraordinary properties that do not exist in natural materials [1]. Because of their unique and attractive properties, they have been applied in various fields, such as perfect lenses [2], cloaking [3], and miniaturized microwave components [4]. Recently, MM absorbers have been proposed in the microwave, terahertz (THz), and infrared spectrum [5–7]. When effective permittivity and permeability of MM are tailed to match the impedance of free space, the reflectance is minimized. The transmitted wave is dissipated with dielectric losses and strong resonance.

The rapid growth of wireless communication and remote sensing applications has created a demand for advances in conventional technologies. Because of this, researchers are attempting to develop highly flexible and reversibly deformable electronic devices and flexible MM absorbers have the potential to open new opportunities, particularly for application in wearable devices and systems. For instance, flexible MM absorbers must be bendable for attachment to nonplanar or curved surfaces [8–10].

Owing to these demands, flexible MM absorbers have been proposed in previous studies. Kim et al. presented a broadband THz absorber on a flexible polydimethylsiloxane (PDMS) substrate [11]. To investigate the performance of the flexible absorber, measurements were taken of the bent absorber at various bending radii. Iwaszczuk et al. demonstrated a broadband THz absorber based on flexible metamaterial film with highly resonant absorption [10]. It can smoothly coat the surface of a cylinder and provide an electromagnetic response to minimize radar cross section (RCS). Singh et al. proposed an ultrathin millimeter wave absorber on a flexible polyimide substrate [8]. The total thickness of the absorber was 126 μm (almost 1/20 of the wavelength), and both single- and dual-band absorbers at resonant frequencies were investigated.

In addition, liquid metal has undergone significant development during the past few years as a new technology with promising applications and unique properties. The main advantages of liquid metal are a high quality factor (when loaded into some resonator or absorber), especially at high frequencies; high fabrication efficiency; and stable fabrication quality. In this work, eutectic gallium indium (EGaIn; 75% Ga, 25% In, by weight) alloy is chosen as the liquid metal [12]. Owing to the low viscosity of EGaIn, it can be easily injected into microfluidic channels at room temperature with pressure to the inlet hole. In addition, EGaIn has a low level of toxicity and a thin, solid-like oxide skin on its surface to improve stability (i.e., it is nonvolatile). Therefore, EGaIn is superior to mercury, which is toxic and forms unstable structures. The oxide layer does not grow thicker with time, and therefore, it can maintain its performance for a long duration. Recently, flexible electronic devices have been realized by using liquid metal. For instance, an unbalanced loop antenna and a half-wave dipole antenna were reported by So et al. and Cheng et al., respectively [12, 13]. These antennas were fabricated by injecting galinstan (Ga 68.5%, In 21.5%, and Sn 10%) and EGaIn into microfluidic channels in elastic PDMS substrates. In addition, a novel multilayer microstrip patch antenna composed of liquid metal was demonstrated by Hayes et al. [14]. The performance of the flexible antennas did not vary significantly when subjected to bending. Although the combination of PDMS substrate and liquid metal has been employed in antenna applications, this technique has not been used for MM absorber applications.

This paper describes the fabrication and characterization of the flexible MM absorber. The flexible MM absorber is developed on a flexible PDMS substrate. Conductive patterns of the proposed flexible MM absorber are realized by liquid metal whereas previous flexible MM absorbers [7–9] were realized by copper or gold for conductive patterns. Liquid metal allows the proposed MM absorber to be deformed significantly and reversibly without loss of electrical continuity, whereas copper or gold fatigues and is destroyed when bent repeatedly.

In order to inject liquid metal for the conductive patterns, an elastomeric microfluidic channel is formed on the PDMS by laser etching. After encapsulating the microfluidic channel by the PDMS, EGaIn is injected into the microfluidic channel. Two PDMS materials are bonded after surface treatment of oxygen plasma [15]. The proposed method can reduce the weight of the package and offers better environmental adaptability (waterproof, flexible, and temperature friendly).

2. Absorber design

The cross ring shape is proposed for a unit cell of the MM absorber as illustrated in Fig. 1. Because the conductive patterns are realized by injecting liquid metal into the microfluidic channel, a long single microfluidic channel is designed, and conductive patterns are connected to each other. Microfluidic channels are engraved onto the PDMS material with thickness of 1 mm. The engraved PDMS material is bonded by another PDMS material as a sealing cap, and the bottom layer is covered by copper tape. The width of the microfluidic channel is decided to be 0.5 mm after considering the viscosity of the liquid metal. The incident wave vector is perpendicular to the pattern plane in the z-axis as shown in Fig. 1(b). The electric field is parallel to the x-axis, and the magnetic field is parallel to the y-axis.
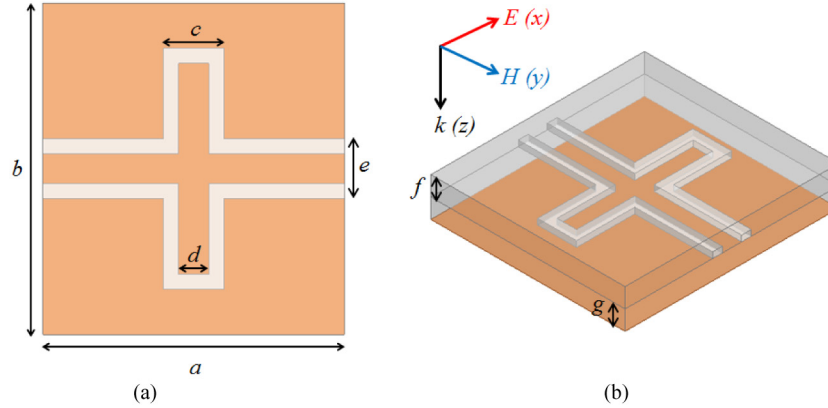

Fig. 1. Layout of the proposed unit cell: $a = 10$ mm, $b = 11$ mm, $c = 2$ mm, $d = 1$ mm, $e = 2$ mm, $f = 1$ mm, $g = 1$ mm; (a) top view; (b) bird view.

A finite-element-method (FEM)-based ANSYS high-frequency structure simulator (HFSS) is used to design an MM unit cell. Absorptivity $A(\omega)$ is calculated from reflection coefficient $\Gamma(\omega)$ and transmission coefficient $T(\omega)$ [5]:

$$A(\omega) = 1 - \Gamma(\omega) - T(\omega) \qquad (1)$$

Therefore, high absorptivity is achieved by zero reflection and transmittance. Because the MM unit cell is a dispersive resonant structure, zero reflection is realized by manipulating its effective permittivity $\varepsilon(\omega)$ and permeability $\mu(\omega)$ at the resonant frequency ω [16]. Zero transmittance is realized by increasing the thickness of a lossy dielectric material because transmitted EM energy must be dissipated from dielectric losses. The final geometrical dimensions of the unit cell are indicated in Fig. 1(a). Under normal incidence, the simulated impedance of the MM unit is plotted in Fig. 2. The impedance $Z_M(\omega)$ is calculated from the S-parameters [17].

$$Z_M(\omega) = \sqrt{\frac{\mu_{rM}\mu_0}{\varepsilon_{rM}\varepsilon_0}} = \eta_0 \sqrt{\frac{(1+S_{11})^2 - S_{21}^2}{(1-S_{11})^2 - S_{21}^2}} \qquad (2)$$

where $\varepsilon_{rM}(\omega)$ and $\mu_{rM}(\omega)$ are the relative permittivity and permeability of the MM unit cell, respectively. ε_0, μ_0, and η_0 represent permittivity, permeability, and intrinsic impedance of

free space, respectively. When $Z_M(\omega)$ is matched to η_0, $\Gamma(\omega)$ becomes zero under normal incidence. It is observed from Fig. 2 that the real part of Z_M is close to 377 Ω, and the imaginary part of Z_M is close to zero at 8.19 GHz. Therefore, it is expected that the proposed MM absorber works at 8.19 GHz.
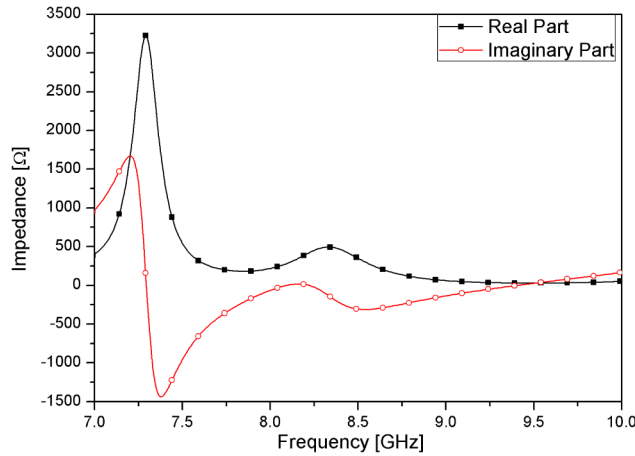

Fig. 2. Complex impedance of the proposed metamaterial absorber.

Figure 3 shows the simulated absorption ratios at *x*- and *y*-polarized electric fields. As expected, perfect absorptivity is achieved at 8.19 GHz at *x*-polarized electric field. On the other hands, the absorptivity at *y*-polarized electric field decreases and additional resonance is observed at 7.53GHz because the proposed MM unit cell is not rotationally symmetric. In addition, the absorptivity of the bent sample at different curvature radii (R) is simulated and compared with the absorptivity of the flat sample. It is observed that the high absorption ratio is kept at both flat and bent absorber. However, the absorption frequency is changed when the absorber is bent as shown in the inset of Fig. 4. Figure 4 shows that the absorption frequencies are 9.15 GHz, 9.15 GHz, and 9.28 GHz when R is 10mm, 20mm and 40mm, respectively. The frequency change is due to the bulky unit cell. In order to make the resonant frequency insensitive to curvature ratio, a subwavelength unit cell needs to be employed.
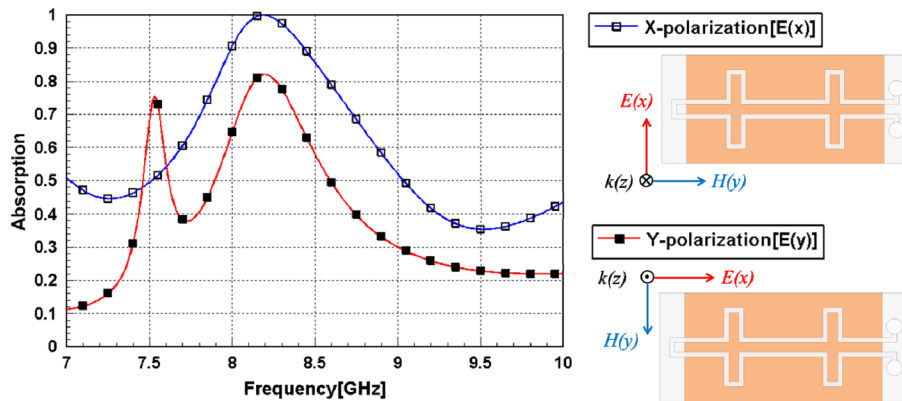

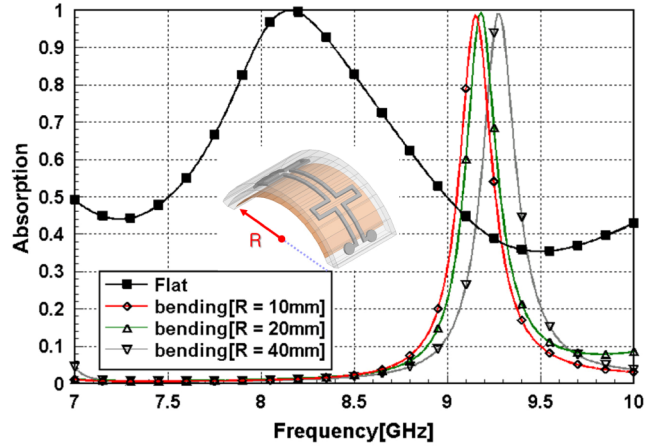Fig. 3. Simulated absorptivity of the proposed MM absorber at different polarizations.

Fig. 4. Simulated absorptivity results of the flat and bent MM absorber with different curvature radii R.

The absorbing mechanism can be understood from field distributions as well. When an EM wave is incident on the MM absorber, the electric field is coupled with the top electric LC (ELC) resonator, which controls $\varepsilon(\omega)$, and the anti-parallel current between the top and bottom layers generates magnetic resonance, which controls $\mu(\omega)$ [16]. Figure 5(a) shows the simulated magnitudes of electric fields in the designed MM absorber at 8.19 GHz. These fields are plotted on the middle of the liquid metal plane. The plane is When an EM wave is incident, a strong electric coupling is generated at each edge of the cross-shaped pattern. In addition, Fig. 5(b) shows the electric vector current distribution. It is observed that currents between the top and bottom layers are antiparallel, which results in magnetic coupling. Therefore, $\varepsilon(\omega)$ can be controlled by the top liquid metal pattern, and $\mu(\omega)$ can be controlled by the thickness of the PDMS material. The volume loss densities are plotted in Fig. 5(c). It is obvious that the total loss is increased by the thicker substrate.
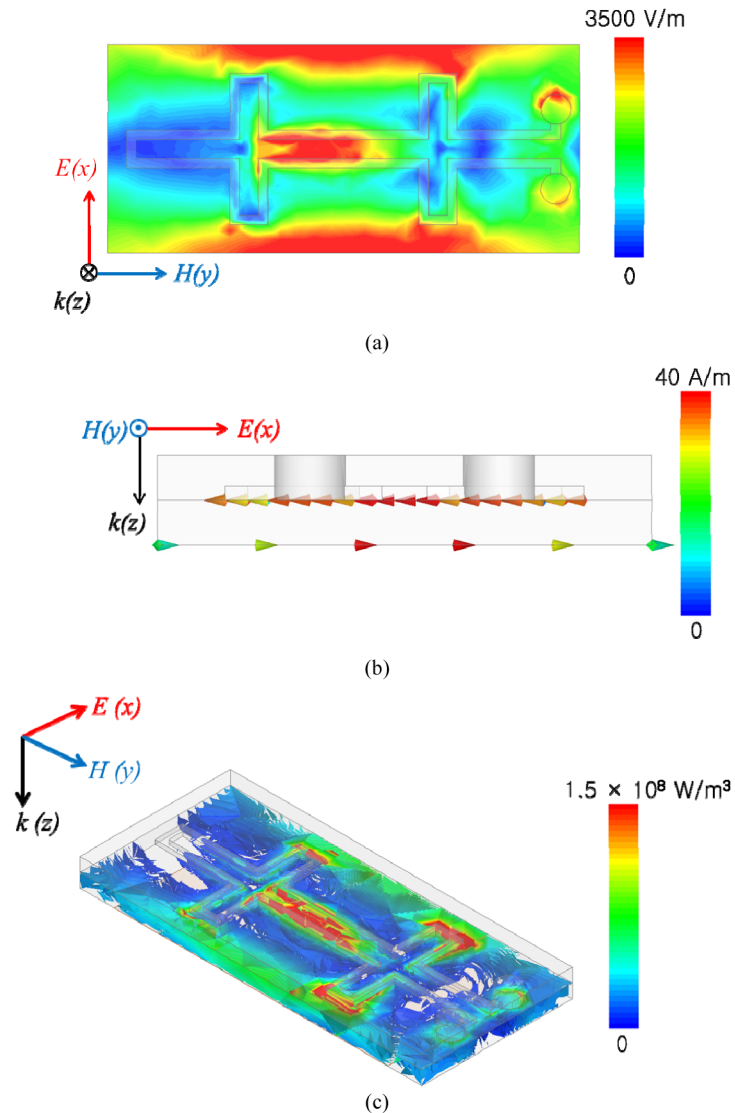
Fig. 5. Simulated field distributions at 8.19 GHz: (a) magnitude of electric field; (b) vector current density; (c) volume loss density.

3. Fabrication and experimental results

Figure 6 shows a schematic diagram of the fabrication process for the proposed flexible MM absorber. First, a microfluidic channel is engraved on the PDMS substrate by laser etching. The fluidic channel has a 0.3 mm height and 0.5 mm width. After laser etching, the PDMS material is exposed to oxygen plasma. The plasma-treated PDMS is enclosed by another plasma-treated plain PDMS material in order to generate the microfluidic channels for the liquid metal. The inlet and outlet are installed on the PDMS substrate, and EGaIn is injected through a syringe. The bottom ground plane is simply realized using copper tape.
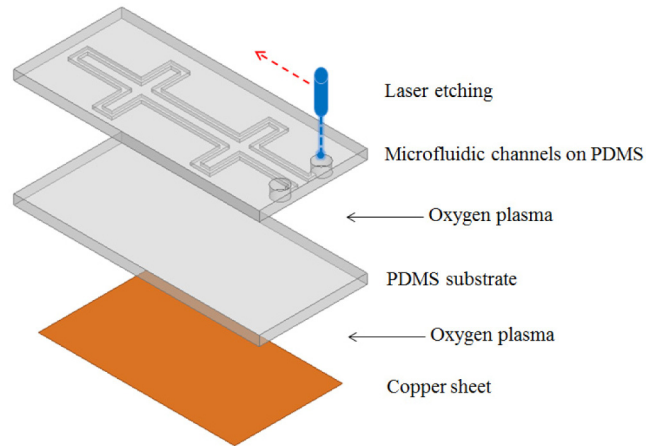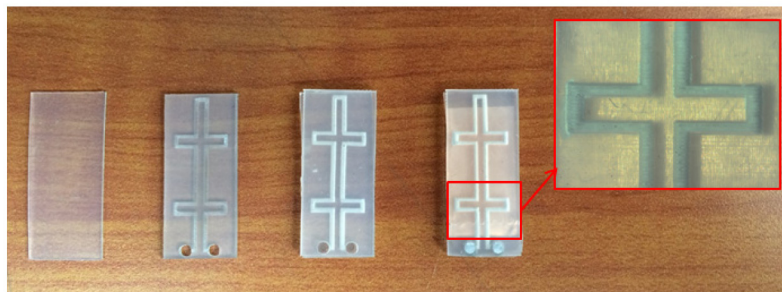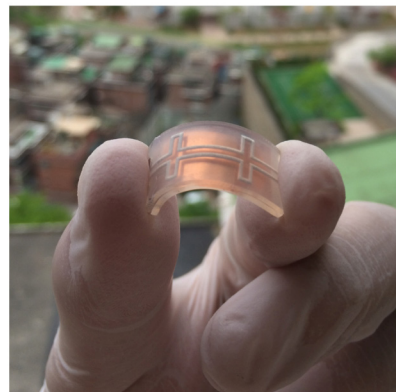
Fig. 6. Illustration of fabrication process.

Figure 7(a) shows pictures of the fabricated prototype at each fabrication step. The first sample is the plain PDMS material, and the second sample is the laser-etched PDMS material. The third sample is the result of bonding the two PDMS materials. The fourth sample is the final MM absorber after injecting the liquid metal. The liquid metal-filled channel is shown in the zoomed-in image (inset). The flexibility of the fabricated MM absorber can be observed in Fig. 7(b).

(a)

(b)

Fig. 7. Illustration of fabricated MM absorber: (a) samples at each fabrication step; (b) bent flexible MM absorber.

The absorptivity of the fabricated flexible MM absorber is tested by the Anritsu MS2038C vector network analyzer as shown in Fig. 8(a) [18]. The MM absorber is inserted between two waveguide-coaxial adaptors. Figure 8(b) shows the open-ended rectangular waveguide, which has an aperture size of 10.22 mm × 22.92 mm for X-band operation. The MM absorber is placed on the aperture as shown in Fig. 8(c).

The absorptivity can be calculated from the reflection and transmission coefficients in Eq. (1). The reflection and transmission coefficients can be measured from S_{11} and S_{21} of the S-parameters, respectively. The transmission coefficient from S_{21} is zero because the back side of the proposed MM absorber is completely covered by copper tape.

Figure 9 shows the simulated and measured absorptivity of the proposed absorber. The measured resonant frequency is 8.22 GHz, and the simulated resonant frequency is 8.19 GHz. Although a slight difference is observed, the simulated and measured results are in good agreement with each other. A frequency shift of 30 MHz is due to error in dielectric constant of the PDMS. At the resonant frequency, almost perfect absorptivity is achieved from both simulation and measurement results.

(a)

(b)

(c)

Fig. 8. (a) Waveguide measurement setup; (b) open-ended rectangular waveguide; (c) sample in the top of the waveguide adaptor.
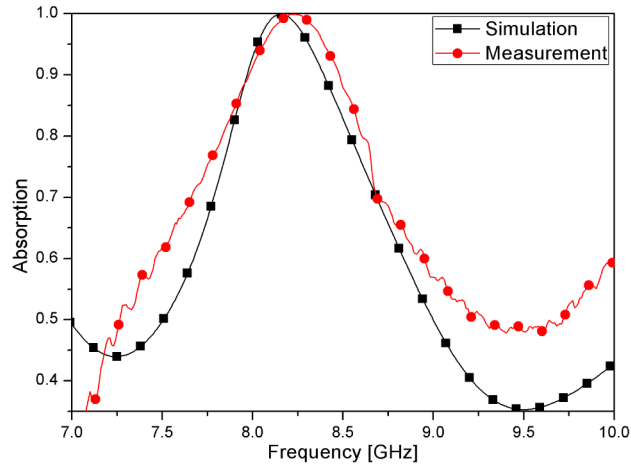
Fig. 9. Simulated and measured absorptivity results.

4. Conclusion

In this paper, a novel concept of the flexible MM absorber is proposed. EGaIn liquid metal is used for conductive patterns for flexibility. Two flexible PDMS materials are used as a supporting substrate and sealing cap, respectively. The liquid metal is enclosed in elastomeric microfluidic channels, which are built after bonding two plasma-treated PDMS materials. The absorptivity of the proposed MM absorber is simulated and measured. At 8.22 GHz, almost perfect absorptivity is achieved from the measurement. The proposed flexible MM absorber can be used for flexible electronics. In addition, it can be used for wireless sensor applications to monitor strain on the surface in real time.

Acknowledgments